Encapsulated Bacillus anthracis interacts closely with liver endothelium.

Alejandro Piris-Gimenez, Jean-Philippe Corre, Gregory Jouvion, Thomas Candela, Huot Khun, Pierre L. Goossens

MAJOR ARTICLE

Encapsulated *Bacillus anthracis* Interacts Closely with Liver Endothelium

Alejandro Piris-Gimenez,[1,2,a] Jean-Philippe Corre,[1,2,a] Gregory Jouvion,[3] Thomas Candela,[1,2] Huot Khun,[3] and Pierre L. Goossens[1,2]

[1]Institut Pasteur, Unité Toxines et Pathogénie Bactériennes, [2]Centre National de la Recherche Scientifique Unité de Recherche Associée 2172, and [3]Institut Pasteur, Unité de Recherche et d'Expertise Histotechnologie et Pathologie, Paris, France

Background. The *Bacillus anthracis* poly-γ-D-glutamate capsule is essential for virulence. It impedes phagocytosis and protects bacilli from the immune system, thus promoting systemic dissemination.

Methods. To further define the virulence mechanisms brought into play by the capsule, we characterized the interactions between encapsulated nontoxinogenic *B. anthracis* and its host in vivo through histological analysis, perfusion, and competition experiments with purified capsule.

Results. Clearance of encapsulated bacilli from the blood was rapid (>90% clearance within 5 min), with 75% of the bacteria being trapped in the liver. Competition experiments with purified capsule polyglutamate inhibited this interaction. At the septicemic phase of cutaneous infection with spores, the encapsulated bacilli were trapped in the vascular spaces of the liver and interacted closely with the liver endothelium in the sinusoids and terminal and portal veins. They often grow as microcolonies containing capsular material shed by the bacteria.

Conclusion. We show that, in addition to its inhibitory effect on the interaction with the immune system, the capsule surrounding *B. anthracis* plays an active role in mediating the trapping of the bacteria within the liver and may thus contribute to anthrax pathogenesis. Because other microorganisms produce polyglutamate, it may also represent a general mechanism of virulence or in vivo survival.

Anthrax is a combination of toxemia and rapidly spreading infection that progresses to septicemia and death [1]. *Bacillus anthracis* produces 2 major virulence factors: toxins and the capsule [2]. The lethal and edema toxins alter host cell signaling and thereby modulate the host immune response [3, 4]. The successful dissemination and survival of *B. anthracis* in the host during infection is dependant on the presence of the capsule [5, 6]. The capsule is exclusively composed of a highly repetitive polymer of poly-γ-D-glutamate (γPDGA). It is produced by the *capBCAE* operon products [7, 8] and is anchored to the bacterial peptidoglycan by the *CapD* gene product [7, 8]. Some γPDGA filaments are released into the external medium or remain noncovalently associated to the *B. anthracis* surface [7]; circulating γPDGA has even been suggested as a marker for immunodiagnosis and the prognosis of anthrax [9].

Some of the mechanisms by which the capsule is able to subvert host defenses were described many years ago. The capsule impedes phagocytosis [10, 11]. The mechanisms of this inhibition are still largely unknown. The capsule is poorly immunogenic and behaves as a thymus-independent type 2 antigen [12]; this is most probably related to the highly repetitive structure, its enantiomeric content, and the γ linkage of the γPDGA filaments [13, 14]. It thus eludes recognition as an antigen by the immune system and protects the other surface antigens by shielding them from the circulating antibodies.

In this study, we hypothesized that the polyglutamate

Received 28 January 2009; accepted 12 June 2009; electronically published 28 September 2009.

[a] Potential conflicts of interest: none reported.

Financial support: Délégation Générale pour l'Armement grant (no. 04.34.025), the Anthrax-Euronet coordination program of the European Commission Sixth Framework Programme, and a Roux fellowship from the Institut Pasteur (to G.J.).

Presented in part: Bacillus—ACT 2007, International Conference on *Bacillus anthracis, Bacillus cereus,* and *Bacillus thuringiensis,* Oslo, Norway, 17–21 June 2007.

[a]A.P.-G. and J.-P.C. contributed equally to this article.

Present affiliations: Institute for Cell and Molecular Biosciences, Newcastle upon Tyne, United Kingdom (T.C.); Centro Nacional de Biotecnología, Consejo Superior de Investigaciones Cientificas, Madrid, Spain (A.P.-G.).

Reprints or correspondence: Dr. Pierre L. Goossens, Unité Toxines et Pathogénie Bactérienne, Institut Pasteur, 28 rue du Dr. Roux, 75724 Paris cedex 15, France (Pierre.Goossens@pasteur.fr).

The Journal of Infectious Diseases 2009; 200:1381–9

0022-1899/2009/20009-0005$15.00
DOI: 10.1086/644506

capsule surrounding *B. anthracis* could interact with host tissue surfaces during infection and thus play an active role in tissue dissemination and potentially in toxin delivery. We show that *B. anthracis* capsule interacts closely with the liver endothelium, trapping the bacteria within this vital organ.

MATERIALS AND METHODS

B. anthracis *strains and mice.* Outbred OF1 female mice (weight, 22–24 g) were purchased from Charles River and housed in the animal facilities of the Institut Pasteur, which is licensed by the French Ministry of Agriculture, in compliance with European regulations. The protocols were approved by the Institut Pasteur Safety Committee according to the standard procedures recommended by the Institut Pasteur Animal Care and Use Committee.

The *B. anthracis* strains used were the Δ*pagA* 9602P (mean lethal dose, <25 spores subcutaneously in mice) [15, 16], and its rough derivative 9602PR cured of the pXO2 plasmid by incubation in a 20% CO_2 atmosphere at 37°C, as described elsewhere [17]; this strain is avirulent, because it lacks *B. anthracis* major virulence factors, capsule, and toxins. Purified spores were prepared as described elsewhere [18]. A bioluminescent derivative of the Δ*pagA* 9602P, expressing the *lux* operon of *Photorhabdus luminescens* under the control of the highly in vivo expressed promoter p*agA*, was also used [19].

Infection experiments. For cutaneous infection with spores, spore suspensions in phosphate buffered saline (PBS; 10 μL) were injected into the ear [19]. For infection with the Δ*pagA* 9602P encapsulated bacilli or the nonencapsulated 9602PR control bacilli, spores were incubated in brain heart infusion (BHI) (Difco) for 5 min to ensure germination, washed, and transferred into R medium supplemented with 0.6% $NaHCO_3$ for 1 h at 37°C with agitation [20, 21]. The presence of capsule for the Δ*pagA* 9602P bacilli was checked by light microscopy with India ink staining. After washing, the bacilli were resuspended in 0.15 M NaCl, and the suspension of bacilli was injected intravenously. Unless otherwise stated, intravenous injection was performed into the caudal vein. In some experiments, to ensure that the maximum of bacteria reached the liver, injection was performed directly into the portal vein in anesthetized animals.

The inoculum size was verified retrospectively by plating 10-fold serial dilutions of the inoculum on BHI agar plates. When indicated, capsule polyglutamate (30 μg), purified as described elsewhere [7, 22], was preinjected into the portal vein 2.5 min before intravenous injection of the encapsulated or control nonencapsulated bacilli into the caudal vein. In some experiments, to eliminate the blood present in the vascular compartment of the liver, liver perfusion was performed as described elsewhere [23].

To determine bacterial loads, liver, spleen, lungs and kidneys were removed, and blood was collected at specific time points after infection. Organs were homogenized in 5 mL of PBS; 10-fold serial dilutions were plated on BHI agar plates, and colony-forming unit (CFU) counts were determined. Results are expressed as mean ± standard error of the mean (SEM) $\log_{10}$ CFU per organ or per mL of blood, with at least 4 animals per group.

Histological analysis. Livers were obtained 22 h after ear subcutaneous inoculation (1×10^4 9602P spores; 8 mice), 6 h after intravenous injection (3.4×10^6 encapsulated bacilli; 2 mice), and 5 min after intraportal injection of 30 μg of capsule polyglutamate (3 mice). The whole livers were fixed in 4% neutral buffered formalin for 1 week, then different sections were realized for the microscopic observation: through (1) the left lateral lobe; (2) the left and right medial lobes, including the gall bladder; and (3) the caudate lobe. The samples were embedded in paraffin, and serial 5-μm sections were cut and stained with hematoxylin and eosin and Gram stains [24]. Encapsulated bacilli were detected by immunohistochemistry, as described elsewhere [25], with use of a rabbit polyclonal antiserum specific for capsule polyglutamate [7].

Blood chemistry analysis. To evaluate the functional repercussion of the infection on the liver, 2 markers for the assessment of hepatocellular injury, alanine aminotransferase (ALT) and aspartate aminotransferase (AST), were assayed in blood samples. Plasma samples were collected from heparin-treated control mice and mice that were infected subcutaneously into the ear with spores of the bioluminescent encapsulated 9602P strain. Sampling was performed when the mice were at the systemic dissemination stage (ie, were displaying bioluminescent spleen, lungs, and liver), between 24 and 33 h after infection. Heparinised blood samples were filtered through a 0.22-μm filter (Millipore) for sterilization. ALT and AST quantification was then performed using the Vet-test 8008 and the corresponding dry slides (Idexx Laboratories).

Statistical tests. Results are expressed as mean values ± SEM. Statistical significance was determined by Student's *t* test, and $P \leq .05$ was considered to be statistically significant.

RESULTS

Rapid clearance of* B. anthracis *from the blood and targeting of the liver. To determine how the capsule interacts with the host tissues to provoke an uncontrolled infection, we inoculated mice intravenously with either encapsulated nontoxinogenic *B. anthracis* bacilli or its nonencapsulated (and thus avirulent) nontoxinogenic derivative bacilli and characterized bacterial clearance from the bloodstream. Blood clearance of nonencapsulated bacilli was rapid, with a mean (±SEM) of 3.4% ±

Table 1. Organ Distribution of Encapsulated and Nonencapsulated *Bacillus anthracis* 5 min after Intravenous Injection

Inoculum	Mean percentage of inoculum ± SEM (no. of animals)			
	Liver	Spleen	Lungs	Kidneys
Encapsulated bacilli (6.38 $\log_{10}$ CFU)	77 ± 6 (18)	10.7 ± 1.7 (12)	2.3 ± 0.5 (12)	0.3 ± 0.1 (12)
Nonencapsulated bacilli (6.36 $\log_{10}$ CFU)	83 ± 2 (6)	8.5 ± 1.8 (6)	1.5 ± 0.2 (6)	0.4 ± 0.2 (6)

NOTE. Mice were injected intravenously in the caudal vein with encapsulated or nonencapsulated bacilli of the 9602P or 9602PR *B. anthracis* strain, respectively. Five minutes after injection, bacterial load was determined in the liver, spleen, lungs, and kidneys. SEM, standard error of the mean.

1.1% of the inoculum ($n = 8$) remaining in the bloodstream 5 min after intravenous inoculation.

On the basis of previous studies of the antiphagocytic role of the capsule [11, 26], it was expected that the encapsulated bacilli would remain as nonphagocytosed free circulating bacteria in the blood for a prolonged period of time. However, bacterial clearance was unexpectedly rapid for the encapsulated bacilli, with only 7.9% ± 1.3% of the inoculum ($n = 18$) remaining in the bloodstream 5 min after intravenous inoculation. The liver retained a major proportion of the inoculated encapsulated bacilli (77% of the recovered bacteria; Table 1). The spleen harbored 10.7%, whereas the bacterial load in the lungs and the kidneys was low (2.3% and 0.3%, respectively). This organ distribution of encapsulated *B. anthracis* bacilli was similar to the distribution observed with nonencapsulated bacteria (Table 1).

Capsule-mediated interaction of* B. anthracis *with the liver. Five minutes after intravenous injection of encapsulated bacilli, the mean bacterial load (±SEM) was 6.15 ± 0.05 $\log_{10}$ bacteria per mL (ie, 1.4×10^6 bacteria) in the liver and 4.92 ± 0.12 $\log_{10}$ bacteria per mL (ie, 8.3×10^4 bacteria) in the blood ($n = 12$). The volume of blood present in the liver vascular spaces is estimated to be ~120 μL per liver [23]; this gives an estimated CFU count of 1×10^4 bacteria in this blood volume, representing only 0.7% of the bacterial load found in the liver. This suggested that the majority of the bacilli in the liver were not free-circulating bacteria in the blood irrigating the liver, raising the possibility that encapsulated *B. anthracis* interacts with the liver tissue. To test this hypothesis, we infected mice intravenously with encapsulated bacilli, either into the caudal vein or directly into the portal vein upstream from the liver, to target the bacteria to the organ. Five minutes after the injection, we eliminated the blood present in the liver vascular spaces through extensive perfusion of the liver. *B. anthracis* CFU were then quantified in perfused and nonperfused livers. As shown in Table 2, perfusion of the liver did not modify the bacterial load in the liver (no statistically significant difference was noted). This result shows that encapsulated *B. anthracis* could not be dislodged from the liver and suggests a close interaction between the encapsulated bacteria and the liver tissue.

A γPDGA capsule completely surrounds the bacilli in vivo. It was thus likely to be responsible for the bacterial retention within the liver tissue. To test this hypothesis, we performed an in vivo competition assay by injecting purified γPDGA into the portal vein 2.5 min before intravenous inoculation (into the caudal vein) of the encapsulated bacilli. Histological analysis

Table 2. Effect of Liver Perfusion on the Liver Bacterial Load

Inoculum, route	Time of perfusion after infection	No. of animals	Bacterial load, mean $\log_{10}$ CFU per liver ± SEM		*P*
			Nonperfused	Perfused	
Encapsulated bacilli (6.33 $\log_{10}$ CFU)					
Intravenous (caudal vein)	5 min	8	5.92 ± 0.04	5.99 ± 0.03	NS
Intravenous (intraportal)	2.5 min	4	6.36 ± 0.06	6.28 ± 0.10	NS
Nonencapsulated bacilli (6.36 $\log_{10}$ CFU)					
Intravenous (caudal vein)	5 min	8	6.32 ± 0.07	6.24 ± 0.06	NS
Spores (4.00 $\log_{10}$ CFU)					
Subcutaneous (ear)	22 h	6	5.87 ± 0.45	5.82 ± 0.30	NS

NOTE. Mice were injected either intravenously with encapsulated (9602P strain) or nonencapsulated (9602PR strain) bacilli or subcutaneously with spores of the encapsulated 9602P strain. Livers were either perfused at the time of removal or not perfused. Livers were then homogenized and the number of CFU per liver determined as described in Materials and Methods. No statistically significant difference was observed between values for nonperfused and perfused livers with use of the Student's *t* test. CFU, colony-forming units; NS, not significant; SEM, standard error of the mean.

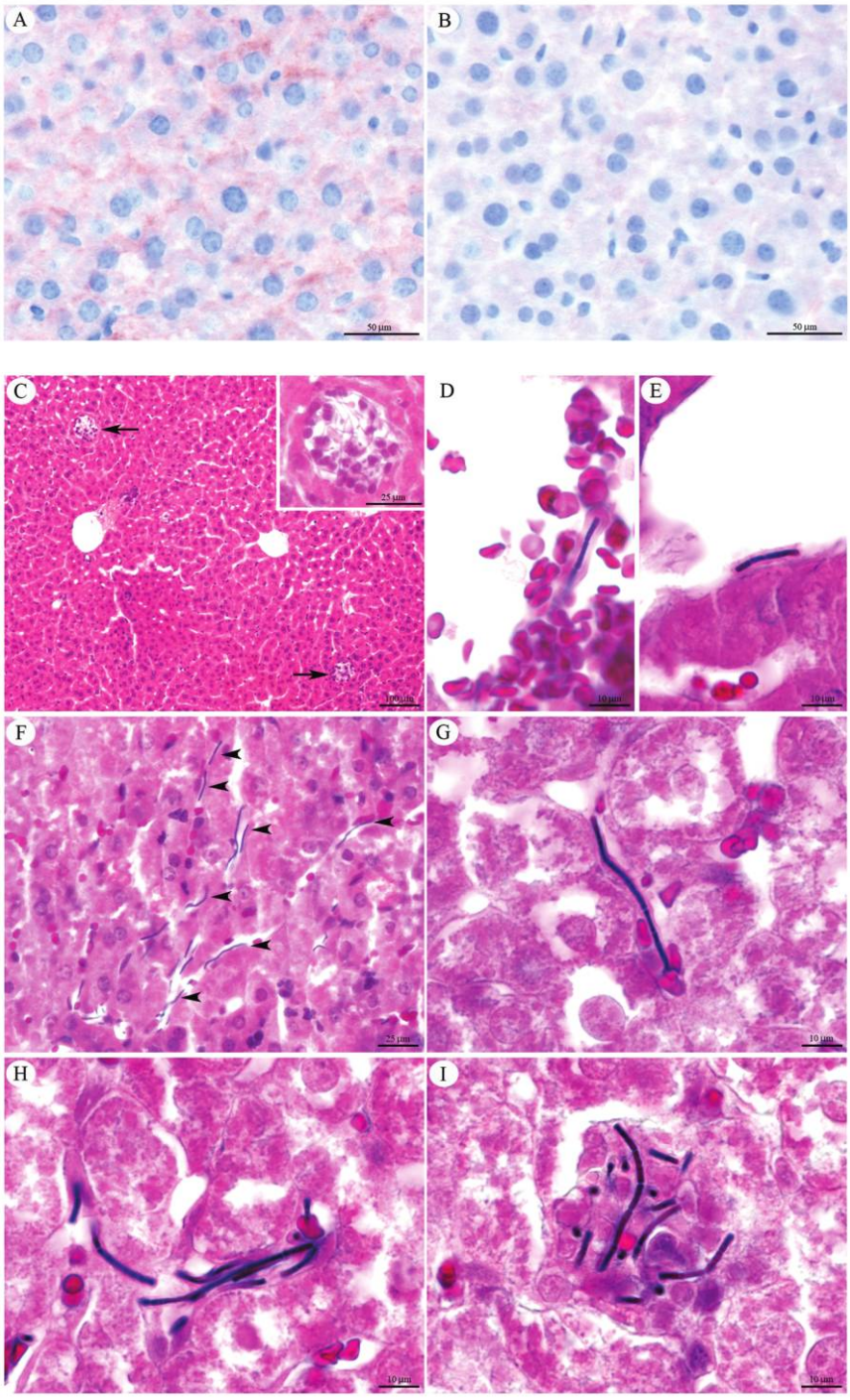

Figure 1. Distribution of poly-γ-D-glutamate injected by intraportal route and histopathology of a 6-h intravenous infection. (*A* and *B*). Poly-γ-D-glutamate (30 μg) was injected directly into the portal vein, and 5 min later, the livers were processed for immunochemistry analysis with a polyclonal antiserum directed against *Bacillus anthracis* capsule polyglutamate *(A)*; control liver is also shown *(B)*. *C–I*, Mice were injected intravenously (via the caudal vein) with encapsulated bacilli (6.53 $\log_{10}$ CFU), and the liver was removed 6 h later for histological analysis. A minimal, multifocal neutrophilic hepatitis was observed, characterized by *(C)* randomly distributed intrasinusoidal infiltrations of neutrophils *(arrows)* resulting in focal dilatations of these sinusoids *(inset)*. Bacteria were mainly located in the vascular spaces. In the central vein, bacteria could be detected in the lumen *(D)* or along endothelial cells *(E)*. In the sinusoids, bacteria were almost always detected in close contact with endothelial cells *(F)*, either alone *(G)* or in small clusters *(H)*. Small groups of bacteria could also be detected in the neutrophilic infiltrates *(I)*. *A* and *B* show immunolabeling counterstained with hematoxylin, *C* shows hematoxylin and eosin staining, and *D–I* show Gram staining.

Table 3. Effect of Purified Poly-γ-D-Glutamate Preinjection on *Bacillus anthracis* Retention within the Liver

Inoculum	Bacterial load, mean $\log_{10}$ CFU per liver ± SEM (no. of animals)		Inhibition[a], %	*P*
	Control group	Capsule competition group		
Encapsulated bacilli (6.89 $\log_{10}$ CFU)	6.42 ± 0.07 (12)	5.96 ± 0.11 (14)	65	.002
Nonencapsulated bacilli (6.49 $\log_{10}$ CFU)	6.61 ± 0.19 (6)	6.62 ± 0.12 (6)	0	NS

NOTE. Mice were injected with purified poly-γ-D-glutamate (30 μg) into the portal vein 2.5 min before intravenous challenge into the caudal vein with either encapsulated bacilli (9602P strain) or nonencapsulated bacilli (9602PR strain). Control mice were challenged without preinjection of capsule polyglutamate. Livers were homogenized 2.5 min after *B. anthracis* injection, and the number of CFU was determined as described in Materials and Methods. Statistical significance was calculated with Student's *t* test. CFU, colony-forming units; NS, not significant.

[a] Percentage of inhibition of *B. anthracis* CFU retained in the liver after capsule competition.

with anti-γPDGA antibodies shows deposits of polyglutamate along the sinusoids (Figure 1A). Preinjection of the γPDGA significantly decreased the encapsulated *B. anthracis* bacterial load within the liver tissue (65% inhibition; Table 3). These observations confirm that encapsulated *B. anthracis* are able to rapidly interact with liver tissue via its capsule.

The specificity of this inhibition was tested by checking the effect of polyglutamate injection on the interaction of the nonencapsulated *B. anthracis* bacilli in the liver. Nonencapsulated bacilli were also trapped in the liver; perfusion of the liver 5 min after intravenous injection of nonencapsulated bacilli did not modify the liver bacterial load (Table 2). In contrast to encapsulated bacilli, the retention of nonencapsulated bacilli was not inhibited by intraportal preinjection of γPDGA (Table 3). These observations show that nonencapsulated *B. anthracis* interact with liver tissue by a mechanism that is different from that by which encapsulated bacilli interact with liver tissue.

We then determined whether initial adhesion of the bacteria within the liver could be a short-term phenomenon. Mice were injected intravenously with encapsulated bacilli, and the bacterial load in the liver was determined at 5 min, 30 min, and 60 min after injection (Figure 2). A 58% decrease was observed between the levels determined at 5 min and 30 min ($P < .001$), but no statistically significant difference existed between levels determined at 30 min and 60 min.

The distribution of the bacteria in the liver was studied 6 h after the intravenous injection of the encapsulated bacilli, at a time when the bacteria could technically be detected by histological analysis. (Figure 1)The livers displayed minimal inflammatory lesions that were multifocal and randomly distributed. They were characterized by focal dilatations of hepatic sinusoids (up to 100 μm in diameter) associated with intrasinusoidal accumulation of neutrophils (Figure 1*C*). Using Gram staining, bacteria could be detected in the vascular spaces, mainly in the central vein (Figure 1*D* and 1*E*) and the sinusoids (Figure 1*F–H*). They were almost always located along endothelial cells (Figure 1*E–H*), either alone (Figure 1*E–G*) or grouped in small clusters (Figure 1*H*). Small clusters of bacteria were also observed in the neutrophil infiltrates (Figure 1*I*).

Close interaction between encapsulated* B. anthracis *and liver endothelium. The experiments described above were performed after intravenous injection of bacilli. This does not represent a natural route of infection. We thus asked whether the interaction between encapsulated *B. anthracis* and liver tissue also occurs during a natural infection. Mice were inoculated subcutaneously with 4 $\log_{10}$ spores of the encapsulated 9602P strain. Twenty-two hours after inoculation, the CFU count was determined in liver and blood specimens. The results that were obtained were similar to those obtained after intravenous infection. The mean (±SEM) bacterial load was 6.3 ± 0.3 $\log_{10}$ bacteria (ie, 2×10^6 bacteria) in liver ($n = 10$) and 5.4 ± 0.4 $\log_{10}$ bacteria per mL (ie, 2.5×10^5 bacteria per mL) in blood

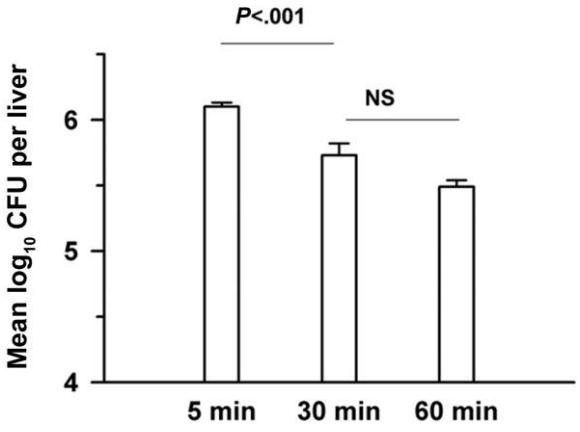

Figure 2. Time course of encapsulated *Bacillus anthracis* retention within the liver after intravenous injection. Encapsulated *B. anthracis* were injected intravenously into 6 mice, and the bacterial load in the liver was determined 5 min, 30 min, and 60 min after perfusion of the liver to eliminate the blood present in the liver vascular spaces. Results are expressed as mean $\log_{10}$ CFU per liver (± standard error of the mean; *whiskers*). Statistical significance was calculated with Student's *t* test and was set at $P < .05$. NS, not significant.

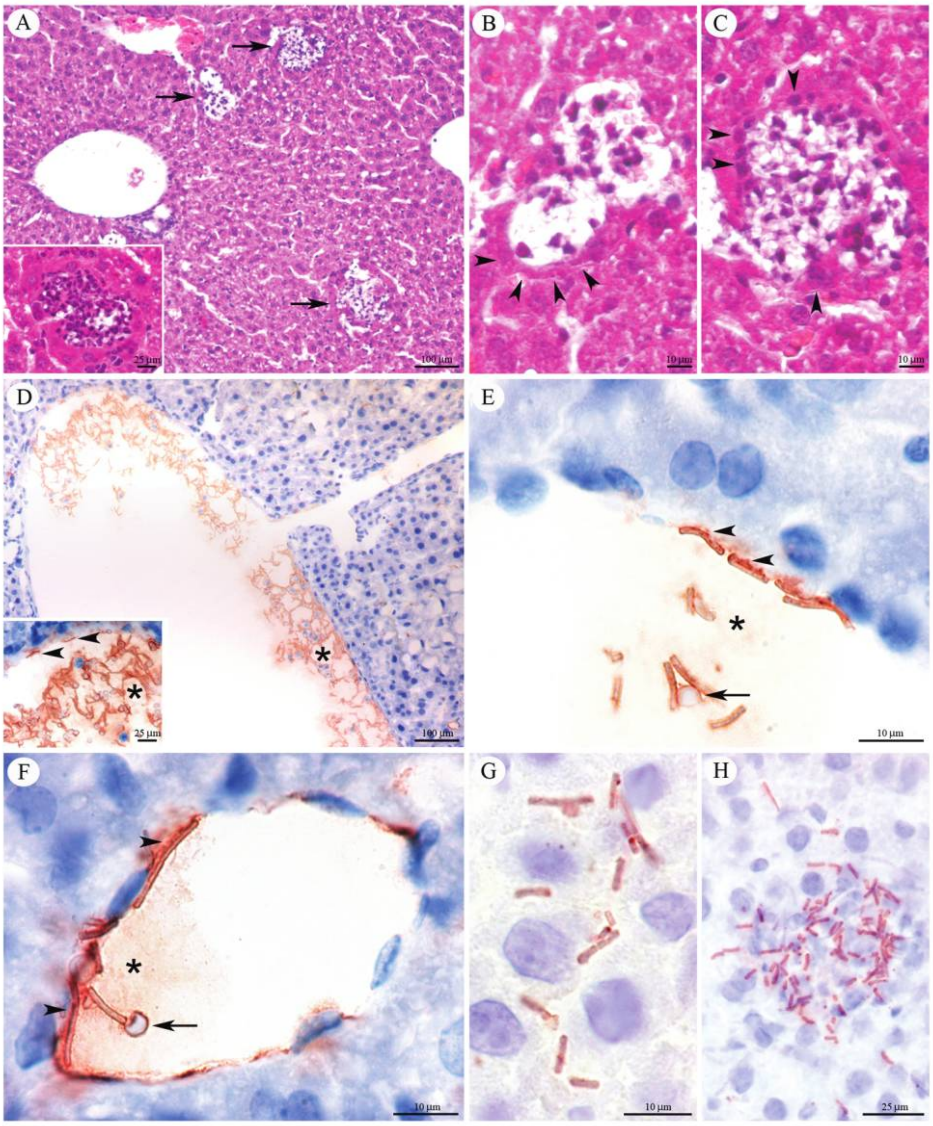

Figure 3. Encapsulated *Bacillus anthracis* interacts closely with liver endothelium. Minimal-to-mild multifocal neutrophilic hepatitis, characterized by *(A)* randomly distributed intrasinusoidal infiltrations of neutrophils *(arrows)* resulting in focal dilatations of these sinusoids, associated with *(B)* pavimentous atrophy of peripheral hepatocytes *(arrowheads)*, some of them *(C)* displaying ischemic necrosis *(arrowheads)*. In a few cases, infiltrates contained a high density of karyorrhectic neutrophils *(A; inset)*. Immunohistochemistry with a polyclonal antiserum directed against *B. anthracis* capsule polyglutamate revealed that the bacteria were located *(D)* inside the vascular compartment (mostly central and portal veins); bacteria either formed intraluminal clusters, within granular amorphous material labeled with the anti-capsule antiserum *(asterisks)*, or were very often found in close contact with endothelial cells *(inset; arrowheads)*. *E–F*, high magnification of the interaction between *B. anthracis* and endothelial cells *(arrowheads)* with granular amorphous material around bacteria *(asterisks)*. Erythrocytes present in these microcolonies may display strong labeling of their surface with the anticapsule antibody *(arrows)*. Numerous bacteria were also present in the sinusoids *(G)* and in the neutrophil infiltrates *(H)*. *A–C*, hematoxylin and eosin staining. *D–H*, immunolabeling counterstained with hematoxylin.

specimens. The number of CFU in the blood volume that is present in the liver (120 μL) is thus estimated at 3×10^4 CFU, representing 1.5% of the bacterial load found in the liver.

To confirm that the encapsulated bacteria interacted with the liver tissue, the infected livers were perfused to remove the blood and the free-circulating bacteria present in the vascular spaces of the liver. The CFU count in perfused livers was not different from that in nonperfused livers (Table 2; no statistically significant difference), which showed that encapsulated *B. anthracis* circulating in the blood at this stage of systemic dissemination were trapped in the liver.

To determine the localization of the bacteria and thus visualize the interaction between encapsulated *B. anthracis* and liver tissue in these spore-infected animals, we studied the dis-

tribution of the encapsulated bacteria within the infected liver and the tissue response (Figure 3). The dynamics of infection, although similar, were not synchronous in all infected mice. At the time of necropsy (22 h), different clinical manifestations were observed, with mice displaying clear clinical signs (ruffled hair and severe apathy) or a clinically normal phenotype.

The hepatic lesions and bacteria distribution were very similar to those observed after intravenous inoculation. The livers displayed minimal-to-mild inflammatory lesions that were multifocal and randomly distributed and were characterized by focal dilatations of hepatic sinusoids; however, they were larger than those observed after intravenous inoculation (up to 200 μm in diameter) and were associated with intrasinusoidal accumulation of neutrophils (Figure 3A). The number of neutrophils in the infiltrates varied greatly, from <20 cells to >100 cells. The larger infiltrates contained a high proportion of neutrophils displaying a fragmented nucleus (Figure 3*A*). Hepatocytes located along the dilated sinusoids displayed a pavimentous atrophy probably attributable to compression by the sinusoid dilatation. Some of them also presented a highly acidophilic cytoplasm and highly basophilic condensed nucleus, indicative of ischemic necrosis (Figure 3*A*).

As after an intravenous inoculation, *B. anthracis* was found in the hepatic vascular spaces, very often in close contact with endothelial cells in the sinusoids, the central veins, and the branches of the portal veins (Figure 3*B–E*); it was also occasionally found in close contact with the hepatic artery endothelium (data not shown). Surprisingly, although numerous bacteria were present in the sinusoids (Figure 3*F*), the inflammatory response was minimal; no inflammatory cells were detected around the bacteria in the majority of vascular spaces. In the central and portal veins, the bacteria were either aligned along the endothelium or formed microcolonies in an amorphous granular material labeled by anti-γPDGA antibodies (Figure 3*B–D*). Erythrocytes were often present in these bacterial microcolonies, their surface labeled by the anti-γPDGA antibodies (Figure 3*C* and 3*D*). No labeling was observed in normal noninfected livers (data not shown).

Despite numerous bacteria and polyglutamate deposits, almost no cellular alterations of the hepatocytes were observed on histological analysis. We checked for early signs of cellular suffering by measuring plasmatic levels of hepatic enzymes AST and ALT. We used a bioluminescent 9602P *B. anthracis* strain to follow in real time the kinetics of infection and to ascertain that the mice were at the systemic dissemination stage at the time that blood samples were taken (bioluminescent spleen, lung, and liver; 24–33 h after infection) [19]. Enzymatic levels were found to be increased when the mice displayed clear clinical signs (2 of 3 mice; AST level, 380 and 533 IU/mL; ALT level, 81 and 120 IU/mL), compared with control values (mean AST level $\pm$ SEM, 225 $\pm$ 37 IU/mL; mean ALT level $\pm$ SEM, 49 $\pm$ 5 IU/mL; $n = 4$). Mice that still displayed a clinically normal phenotype had mean AST and ALT values ($\pm$SEM) in the normal range (AST level, 226 $\pm$ 22 IU/mL; ALT level, 53 $\pm$ 8 IU/mL; $n = 4$); from our published and unpublished data, mice at this stage would nevertheless die in <5 h [19]. Because death occurs extremely rapidly, biological signs of hepatic failure are detectable only at the terminal stage.

DISCUSSION

In this study, we show that, in addition to its recognized antiphagocytic and nonimmunogenic properties, the γPDGA capsule surrounding *B. anthracis* mediates close interactions between the encapsulated bacteria and liver endothelium, leading to retention of the bacteria in the liver. The mechanism underlying this interaction was extremely efficient, as shown by the rapid clearance of the encapsulated bacteria from the blood. The bacteria remained in the vascular spaces closely associated with the vascular endothelium. They formed microcolonies containing capsule polyglutamate. This substance could play a role in protecting these bacteria against potentially bactericidal cellular or soluble components of the immune system [26, 27] or in impeding antibiotic diffusion during therapeutic intervention. It could also provide a favorable microenvironment for the multiplying bacteria by retaining salts and nutrients.

Capsular polyglutamate is naturally released during infection through the action of CapD [7, 28, 29]. A recent report has suggested that detection of γPDGA in the serum and urine could assist in the diagnosis and prognosis of anthrax infection [9]. By studying the pharmacokinetics of intravenously injected γPDGA, thus mimicking natural shedding during infection, Sutherland et al [9] showed rapid clearance of γPDGA, with a half-life of <0.13 h for low doses. The authors also observed preferential accumulation along the hepatic sinusoidal endothelium.

In our study, we show that the anchored capsule, by mediating retention of bacteria in the liver, provides an additional virulence mechanism for *B. anthracis*. It is considered that the bacteria reach the blood from the initial infection site through the lymphatic system [1] and initially colonize the spleen [19]. Interestingly, the splenic vein connects with the portal vein, which irrigates the liver. Bacilli exiting from the spleen will thus be retained in the liver through interaction of the polyglutamate capsule with the liver endothelium.

In wild-type strains of *B. anthracis*, which are both encapsulated and toxin-producing, such capsule-mediated focalization of toxin secretion would be expected to increase the local concentration of toxins, leading to targeted toxic activity and liver dysfunction. Indeed, in the clinical reports of the 2001 anthrax attack [30], 9 of the 10 patients infected by means of inhalation had elevated hepatic enzymes at hospital admission.

Bacilli were found in the liver of 3 of 4 patients in another study [31] and in experimentally infected monkeys [32]. Liver lesions have also been observed in infections with the toxin-producing nonencapsulated Sterne strain in A/J mice [33]. Among the reported systemic effects, injection of pure lethal and edema toxins into the vascular system in mice leads to liver dysfunction, as indicated by increased hepatic transaminase levels and decreased serum protein levels [3, 34, 35]. Targeted secretion of lethal toxin along the liver endothelium may thus increase the toxic effects reported by Moayeri et al [35]: hypoxia, vascular damage, and hepatocyte necrosis. Furthermore, the hepatic vascular system has the characteristic of being a portal vascular system (ie, the major part of the entering blood flow is venous, with a low oxygen content). Capsule deposits on the endothelia may interfere with oxygen exchange, further lowering an already reduced oxygen content and thus acting synergistically with lethal toxin to increase local hypoxia [35].

The retention of nonencapsulated *B. anthracis* in the liver was not inhibited by injection of γPDGA. The mechanisms underlying retention of nonencapsulated bacilli are thus different from those observed for encapsulated bacilli. Indeed, because of the absence of the capsule, potential bacterial surface adhesins are in direct contact with the cellular environment (eg, S-layer, surface proteins, and glycoconjugates [36, 37]). One of the consequences of this initial adhesion step would be phagocytosis by macrophages, because the bacteria are not protected by a capsule. Nonencapsulated *B. anthracis* are readily phagocytosed by macrophages or dendritic cells [11, 26]. This is in keeping with many studies involving other nonencapsulated gram-positive and gram-negative bacteria that have shown efficient phagocytosis by phagocytic cells [38–40]. However, during natural infection, *B. anthracis* is encapsulated. It produces its major virulence factors—the toxins and capsule—in the host tissues. We have previously shown, with use of bioluminescent bacteria, that the patterns of dissemination for encapsulated and nonencapsulated *B. anthracis* are markedly different from one another [19, 41]. The presence of the polyglutamate capsule thus modifies the in vivo interactions between the bacteria and tissues [19, 41].

Among other organisms that produce polyglutamate filaments [13], *Staphyloccocus epidermidis* is one of the major cause of hospital-acquired infection, leading to chronic infection as a result of biofilm formation and frequent antibiotic resistance [42]. The polyglutamate attached to the bacterial surface was shown to be critical for virulence in a murine experimental model, probably by protecting the bacteria against antimicrobial peptides and neutrophil phagocytosis [42]. The gram-negative pathogen *Francisella tularensis* has also been shown to possess a polyglutamate synthesis locus that is essential for virulence [43]. Polyglutamate exposed on the surface of microorganisms or shed in the extracellular milieu could thus be a general mechanism of virulence.

In conclusion, we show that, in addition to its inhibitory effect on the interaction with the immune system, the capsule surrounding *B. anthracis* plays an active role in mediating the trapping of bacteria within the liver. This interaction represents a new mechanism by which *B. anthracis* colonizes its host and potentially plays a role in the pathogenesis of anthrax through the localized secretion of toxins or toxic components.

Acknowledgments

We thank Agnès Fouet for many helpful and stimulating discussions and critical reading of the manuscript; Xavier Montagutelli and Laurent Guillemot for their precious help with the blood chemistry analysis; Michèle Mock for her critical interest, encouragement, and constant scientific and material support for this work; and Michel R. Huerre for his invaluable help, advice, and constructive comments regarding the histopathologic characterization and for his continuous support.

References

1. Dixon TC, Meselson M, Guillemin J, Hanna PC. Anthrax. N Engl J Med **1999**; 341:815–26.
2. Mock M, Fouet A. Anthrax. Annu Rev Microbiol **2001**; 55:647–71.
3. Moayeri M, Leppla SH. The roles of anthrax toxin in pathogenesis. Curr Opin Microbiol **2004**; 7:19–24.
4. Tournier JN, Quesnel-Hellmann A, Cleret A, Vidal DR. Contribution of toxins to the pathogenesis of inhalational anthrax. Cell Microbiol **2007**; 9:555–65.
5. Welkos SL, Vietri NJ, Gibbs PH. Non-toxigenic derivatives of the Ames strain of *Bacillus anthracis* are fully virulent for mice: role of plasmid pX02 and chromosome in strain-dependent virulence. Microb Pathog **1993**; 14:381–8.
6. Drysdale M, Heninger S, Hutt J, Chen Y, Lyons CR, Koehler TM. Capsule synthesis by *Bacillus anthracis* is required for dissemination in murine inhalation anthrax. Embo J **2005**; 24:221–7.
7. Candela T, Fouet A. *Bacillus anthracis* CapD, belonging to the gamma-glutamyltranspeptidase family, is required for the covalent anchoring of capsule to peptidoglycan. Mol Microbiol **2005**; 57:717–26.
8. Candela T, Mock M, Fouet A. CapE, a 47-amino-acid peptide, is necessary for *Bacillus anthracis* polyglutamate capsule synthesis. J Bacteriol **2005**; 187:7765–72.
9. Sutherland MD, Thorkildson P, Parks SD, Kozel TR. In vivo fate and distribution of poly-gamma-D-glutamic acid, the capsular antigen from *Bacillus anthracis*. Infect Immun **2008**; 76:899–906.
10. Zwartouw HT, Smith H. Polyglutamic acid from *Bacillus anthracis* grown in vivo; structure and aggressin activity. Biochem J **1956**; 63: 437–42.
11. Makino S, Uchida I, Terakado N, Sasakawa C, Yoshikawa M. Molecular characterization and protein analysis of the *cap* region, which is essential for encapsulation in *Bacillus anthracis*. J Bacteriol **1989**; 171: 722–30.
12. Wang TT, Lucas AH. The capsule of *Bacillus anthracis* behaves as a thymus-independent type 2 antigen. Infect Immun **2004**; 72:5460–3.
13. Candela T, Fouet A. Poly-gamma-glutamate in bacteria. Mol Microbiol **2006**; 60:1091–8.
14. Gill TJ 3rd, Gould HJ, Doty P. Role of optical isomers in determining the antigenicity of synthetic polypeptides. Nature **1963**; 197:746–7.
15. Brossier F, Levy M, Mock M. Anthrax spores make an essential contribution to vaccine efficacy. Infect Immun **2002**; 70:661–4.

16. Berthier M, Fauchere JL, Perrin J. Fulminant meningitis due to *Bacillus anthracis* in 11-year-old girl during Ramadan. Lancet **1996**; 347:828.
17. Sylvestre P, Couture-Tosi E, Mock M. Polymorphism in the collagen-like region of the Bacillus anthracis BclA protein leads to variation in exosporium filament length. J Bacteriol **2003**; 185:1555–63.
18. Sylvestre P, Couture-Tosi E, Mock M. A collagen-like surface glycoprotein is a structural component of the *Bacillus anthracis* exosporium. Mol Microbiol **2002**; 45:169–78.
19. Glomski IJ, Piris-Gimenez A, Huerre M, Mock M, Goossens PL. Primary involvement of pharynx and peyer's patch in inhalational and intestinal anthrax. PLoS Pathog **2007**; 3:e76.
20. Ristroph JD, Ivins BE. Elaboration of *Bacillus anthracis antigens* in a new, defined culture medium. Infection and Immunity **1983**; 39:483–6.
21. Sirard JC, Mock M, Fouet A. The three *Bacillus anthracis* toxin genes are coordinately regulated by bicarbonate and temperature. J Bacteriol **1994**; 176:5188–92.
22. Hanby WE, Rydon HN. The capsular substance of *Bacillus anthracis*: With an appendix by P. Bruce White. Biochem J **1946**; 40:297–309.
23. Goossens PL, Marchal G, Milon G. Early influx of *Listeria*-reactive T lymphocytes in liver of mice genetically resistant to listeriosis. J Immunol **1988**; 141:2451–5.
24. Prophet E, Mills B, Arrington J. Methods in Histotechnology. Washington: AFIP, **1992**.
25. Ristow P, Bourhy P, da Cruz McBride FW, et al. The OmpA-like protein Loa22 is essential for leptospiral virulence. PLoS Pathog **2007**; 3:e97.
26. Keppie J, Smith H, Harris-Smith PW. The chemical basis of the virulence of *Bacillus anthracis*. II. Some biological properties of bacterial products. Br J Exp Pathol **1953**; 34:486–96.
27. Scorpio A, Chabot DJ, Day WA, et al. Poly-gamma-glutamate capsule-degrading enzyme treatment enhances phagocytosis and killing of encapsulated *Bacillus anthracis*. Antimicrob Agents Chemother **2007**; 51: 215–22.
28. Makino S, Watarai M, Cheun HI, Shirahata T, Uchida I. Effect of the lower molecular capsule released from the cell surface of *Bacillus anthracis* on the pathogenesis of anthrax. J Infect Dis **2002**; 186:227–33.
29. Kozel TR, Murphy WJ, Brandt S, et al. mAbs to *Bacillus anthracis* capsular antigen for immunoprotection in anthrax and detection of antigenemia. Proc Natl Acad Sci U S A **2004**; 101:5042–7.
30. Jernigan JA, Stephens DS, Ashford DA, et al. Bioterrorism-related inhalational anthrax: the first 10 cases reported in the United States. Emerg Infect Dis **2001**; 7:933–44.
31. Guarner J, Jernigan JA, Shieh WJ, et al. Pathology and pathogenesis of bioterrorism-related inhalational anthrax. Am J Pathol **2003**; 163: 701–9.
32. Vasconcelos D, Barnewall R, Babin M, et al. Pathology of inhalation anthrax in cynomolgus monkeys (*Macaca fascicularis*). Lab Invest **2003**; 83:1201–9.
33. Duong S, Chiaraviglio L, Kirby JE. Histopathology in a murine model of anthrax. Int J Exp Pathol **2006**; 87:131–7.
34. Firoved AM, Miller GF, Moayeri M, et al. *Bacillus anthracis* edema toxin causes extensive tissue lesions and rapid lethality in mice. Am J Pathol **2005**; 167:1309–20.
35. Moayeri M, Haines D, Young HA, Leppla SH. *Bacillus anthracis* lethal toxin induces TNF-α-independent hypoxia-mediated toxicity in mice. J Clin Invest **2003**; 112:670–82.
36. Mesnage S, Tosi-Couture E, Mock M, Gounon P, Fouet A. Molecular characterization of the *Bacillus anthracis* main S-layer component: evidence that it is the major cell-associated antigen. Mol Microbiol **1997**; 23:1147–55.
37. Mignot T, Mock M, Fouet A. A plasmid-encoded regulator couples the synthesis of toxins and surface structures in *Bacillus anthracis*. Mol Microbiol **2003**; 47:917–27.
38. Gregory SH, Sagnimeni AJ, Wing EJ. Bacteria in the bloodstream are trapped in the liver and killed by immigrating neutrophils. J Immunol **1996**; 157:2514–20.
39. Pluddemann A, Mukhopadhyay S, Gordon S. The interaction of macrophage receptors with bacterial ligands. Expert Rev Mol Med **2006**; 8:1–25.
40. Savina A, Amigorena S. Phagocytosis and antigen presentation in dendritic cells. Immunol Rev **2007**; 219:143–56.
41. Glomski IJ, Corre JP, Mock M, Goossens PL. Noncapsulated toxinogenic *Bacillus anthracis* presents a specific growth and dissemination pattern in naive and protective antigen-immune mice. Infect Immun **2007**; 75:4754–61.
42. Kocianova S, Vuong C, Yao Y, et al. Key role of poly-gamma-DL-glutamic acid in immune evasion and virulence of *Staphylococcus epidermidis*. J Clin Invest **2005**; 115:688–94.
43. Su J, Yang J, Zhao D, Kawula TH, Banas JA, Zhang JR. Genome-wide identification of Francisella tularensis virulence determinants. Infect Immun **2007**; 75:3089–101.